

## Resistive $g$ -modes in a reversed-field pinch plasma

This article has been downloaded from IOPscience. Please scroll down to see the full text article.

2010 Nucl. Fusion 50 052001

(<http://iopscience.iop.org/0029-5515/50/5/052001>)

View [the table of contents for this issue](#), or go to the [journal homepage](#) for more

Download details:

IP Address: 150.178.99.172

The article was downloaded on 28/04/2010 at 11:53

Please note that [terms and conditions apply](#).

## LETTER

# Resistive $g$ -modes in a reversed-field pinch plasma

M. Zuin<sup>1</sup>, S. Spagnolo<sup>1,2</sup>, R. Paccagnella<sup>1</sup>, E. Martines<sup>1</sup>,  
R. Cavazzana<sup>1</sup>, G. Serianni<sup>1</sup>, M. Spolaore<sup>1</sup> and N. Vianello<sup>1</sup>

<sup>1</sup> Consorzio RFX, Associazione EURATOM-ENEA sulla Fusione, 35127 Padova, Italy

<sup>2</sup> Dipartimento di Fisica 'G. Galilei', Università degli Studi di Padova, 35131 Padova, Italy

Received 9 December 2009, accepted for publication 31 March 2010

Published 23 April 2010

Online at [stacks.iop.org/NF/50/052001](http://stacks.iop.org/NF/50/052001)

## Abstract

The first direct experimental evidence of high frequency, high toroidal mode number magnetic fluctuations due to unstable resistive interchange modes ( $g$ -modes) resonant in the edge region of a RFX-mod reversed-field pinch device is presented. Experimental characterization of time and space periodicities of the modes is provided by means of highly resolved in-vessel edge and insertable magnetic diagnostics. Although the saturated energy spectrum of the measured modes is expected to be highly nonlinear, it is found that the spectral mode properties are in good agreement with the predictions of a simple linear resistive magnetohydrodynamic stability analysis. Also a simple quasi-linear saturation model is proposed to explain the observed mode amplitudes.

**PACS numbers:** 52.25.Xz, 52.30.Cv, 52.35.Py, 52.55.Hc, 52.65.Kj, 52.70.Ds

(Some figures in this article are in colour only in the electronic version)

Magnetohydrodynamic (MHD) instabilities and turbulence of interchange nature are ubiquitous in astrophysical [1, 2], magneto-sphere/magneto-tail [3–5] and laboratory plasmas of very different nature from simple toroidal devices [6], to spherical-tokamaks [7], stellarators [8] and field reversed configurations [9]. In fusion oriented magnetically confined plasmas, interchange modes (also known as  $g$ -modes) can cause significant energy and particle transport across the magnetic field. In tokamak plasmas  $g$ -modes are counteracted by shaping and curvature effects of the mean field. The remaining turbulence is therefore of ballooning nature [10] being especially concentrated in the unfavourable toroidal curvature region. For example, ballooning modes are believed to play a role in the formation of edge localized modes (ELMs) [11]. In the reversed-field pinch (RFP) [12] the average edge curvature is unfavourable, the field lines being mainly in the poloidal direction, therefore interchange modes should be expected. According to Suydam's criterion [13], the effect of unfavourable curvature can be mitigated by enhancing the magnetic shear, and this is particularly relevant for RFPs. However, finite plasma resistivity can give rise to a resistive interchange branch of instabilities, resistive  $g$ -modes, that can be destabilized well below Suydam's limit. In the existing literature  $g$ -modes have often been envisaged to be linearly unstable and considered responsible for magnetic field

ergodization and enhanced diffusion and transport in RFP plasmas [14–17]. Recently, the role of resistive  $g$ -modes on the energy confinement time in ohmically heated RFPs has been investigated by a self-consistent transport model taking into account thermal conductivity [18, 19], and a possible way to reduce the growth rate of these kinds of modes along with that of tearing modes by means of the current profile control techniques has been proposed [20]. Some experimental results on the subject are described in [21].

In this letter, we present the first clear experimental evidence of the existence, within the magnetic spectrum, of resistive  $g$ -modes characterized by high mode numbers ( $n > 20$ ) along with a first direct comparison with modelling prediction. We emphasize that our experimental setting is particularly sophisticated and it deals with a large number of electromagnetic signals obtained from in-vessel detectors. We think that a similar complexity of the diagnostic system is mandatory also in other magnetic confinement devices to clearly identify this branch of MHD instabilities. We admit, however, that in higher temperature less collisional devices, such as tokamaks, a simple MHD linear theory could be hardly used for mode identification, at least for operation well below the ideal stability  $\beta$  limits.

The experimental activity described here has been performed on RFX-mod [22, 23], the largest operating toroidal

RFP device (major radius  $R = 2$  m, minor radius  $a = 0.459$  m). Hydrogen is the working gas and the plasma current  $I_p$  spans between 0.3 and 1.8 MA. The electron temperature  $T_e$  at the highest plasma current exceeds on axis 1 keV, while the volume averaged electron density  $n_e$  is in the range  $(1-10) \times 10^{19} \text{ m}^{-3}$ . The discharge duration is up to 0.5 s. The analysis is performed on a large number of discharges ( $\sim 1000$ ) with a reversal parameter, defined as  $F = B_\phi(a)/\langle B_\phi \rangle$  ( $B_\phi(a)$  and  $\langle B_\phi \rangle$  toroidal field at the wall and toroidal field averaged over the plasma cross-section, respectively), in the range  $[-0.5, 0]$ , which corresponds to the edge safety factor  $q(a) \in [-0.07, 0]$ . The plasma is ohmically heated and the loop voltage is in the range 20–40 V, which gives to the RFP the attractive feature of being able to use only ohmic heating also under fusion-relevant conditions. In the RFX-mod device the magnetic boundary is determined by a thin Cu shell, with a vertical field penetration time of around 50 ms, located at  $r/a \cong 1.12$ , and by a system of 192 active saddle coils, supervised by a digital feedback system, fully covering the machine with the aim of controlling the radial fields due to field errors and MHD modes [22]. In the experiments described here the mesh of saddle coils has been used in the so-dubbed clean-mode-control (CMC) configuration, in which the flux through each sensor loop is controlled by the corresponding active coil after performing the two-dimensional fast Fourier transform (FFT) of  $B_r$  and  $B_\phi$  measurements and computing a real time correction of the aliasing of the sideband harmonics generated by the discrete saddle coils [24].

Magnetic fluctuations have been measured by two different highly space- and time-resolved systems of in-vessel magnetic probes: the first is an insertable edge probe, used to investigate high order toroidal harmonics ( $|n| \leq 85$ ), and the second consists of arrays of probes, covering the full toroidal and poloidal angles of the torus. The insertable probe, named *U-probe* [26], which was used in a set of experiments performed at low toroidal plasma currents ( $I_p \leq 500$  kA), consists of two boron nitride cases, 5 cm toroidally spaced, radially inserted from the vacuum chamber up to  $r/a \approx 0.9$  at  $\theta = 0^\circ$  (defined on the equatorial plane on the low field side of the machine with positive  $\theta$  pointing in the upward direction), without significant perturbation of the plasma. Each case contains, along with a number of electrostatic pins, a radial array of 7 three-axial magnetic pick-up coils measuring the time derivative of the three components of the magnetic field ( $\dot{B}_r, \dot{B}_\theta, \dot{B}_\phi$ ). The sampling frequency is 10 MHz, with a bandwidth up to 3 MHz.

The second system of probes is a subset of the ISIS (Integrated System of Internal Sensors) diagnostics [25], a large set of high frequency electrostatic and magnetic probes located inside the vacuum vessel. The magnetic probes consist of coils measuring  $\dot{B}_\phi$ , placed at  $r/a = 1.03$  behind the graphite tiles which cover the first wall of the machine. The probes used in this study are distributed in two different arrays: the first consists of 48 coils evenly distributed in the toroidal direction located at  $\theta = 250^\circ$ ; the second one is a poloidal array, made of 8 equally spaced coils. The sampling frequency for the magnetic measurements from the ISIS system is 2 MHz. The bandwidth of the measurements is up to 400 kHz. The two arrays allow a resolution of the toroidal and poloidal mode numbers  $n$  and  $m$  up to 24 and 4, respectively.

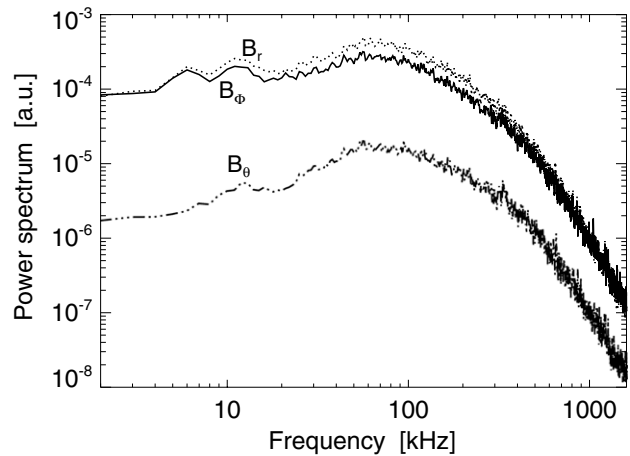


**Figure 1.** Typical power spectra of the time derivative of the three components of the magnetic field, measured by one of the three-axial coils housed in the *U-probe*.

In figure 1 the typical power spectra of the signals from the three components of the magnetic field fluctuations ( $\dot{B}_r, \dot{B}_\theta, \dot{B}_\phi$ ), taken with the *U-probe* in a deeply reversed ( $q(a) \approx -0.04$ ) discharge, are shown. The spectra show that the highest fluctuation levels are present in the ( $\dot{B}_r, \dot{B}_\phi$ ) signals, which correspond to the perpendicular components at the edge of the RFP configuration, where the dominant magnetic field is  $B_\theta$ . The spectra show that large magnetic fluctuations are present for frequencies up to about 200 kHz, with about 60% of the total magnetic fluctuating energy concentrated in the frequency region spanning from 30 to 150 kHz. The space-time properties of the magnetic fluctuations were obtained by Fourier decomposing the signals coming from the complete toroidal array of coils measuring  $\dot{B}_\phi$ . In figure 2 the frequency spectrum of each toroidal Fourier component, here named the  $S(n, f)$  spectrum, is plotted in a colour-coded plot under two different experimental operating conditions, corresponding to plasma equilibria characterized by the  $q$  profiles plotted in figure 2(c). The  $q$  profiles are deduced by using a suitable magnetic profile reconstruction (see for example [27]), which uses external measurements as boundary condition. Each of the spectra was obtained as an average over about 200 discharges. Figure 2(a) was obtained by analysing data taken in a set of discharges with deep reversal of the toroidal magnetic field ( $q(a) \approx -0.05$ ); the  $S(n, f)$  spectrum exhibits the excitation of coherent magnetic fluctuations, in the form of a broad peak, at frequencies above 30 kHz and high ( $n$  up to 50) positive toroidal mode numbers (in the RFX-mod convention, negative and positive  $n$  values refer to modes resonant inside and outside the reversal surface, respectively). It is worth noting that due to the limited ( $|n| \leq 24$ ) spatial resolution of the toroidal array of coils, the computed  $S(n, f)$  spectra were originally affected by aliasing (that is, negative  $n$  values were obtained) and had to be corrected ( $n = n_{<0} + 48$ ). This operation was made possible by a comparison with the  $S(n, f)$  spectra deduced by applying the two-point technique [30] to the signals from the closely spaced magnetic coils of the *U-probe*, which shows that the observed peak actually corresponds to high positive  $n$  values.

The analysis of the poloidal periodicities of the magnetic signals from the poloidal array of coils reveals a clear  $m = 1$

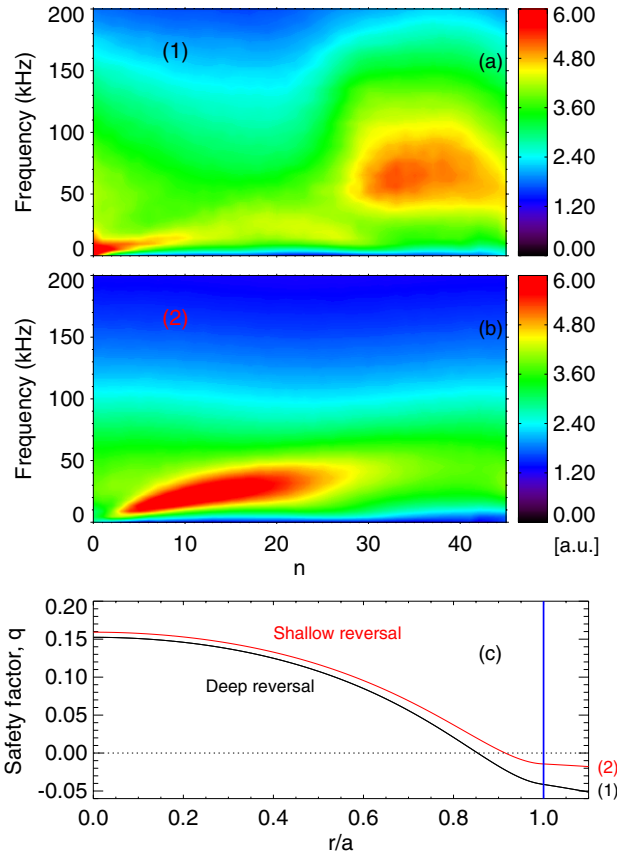


**Figure 2.** Typical colour coded contour plot of the  $S(n, f)$  spectra of magnetic fluctuations for two different experimental conditions: (a)  $S(n, f)$  spectrum obtained at  $q(a) \approx -0.05$ ; (b)  $S(n, f)$  spectrum obtained at shallower reversal of the magnetic field ( $q(a) \approx -0.015$ ); (c) the two reference  $q(r)$  profiles (the vertical line marks the plasma edge). In the sets of discharges considered  $300 \text{ kA} < I_p < 600 \text{ kA}$ .

nature of the magnetic fluctuations in the frequency range above 30 kHz. This  $m = 1$  ‘coherent’ activity, which is the object of the investigation described here, is characteristic of deeply reversed discharges ( $F \leq -0.12$ ). As a confirmation of this, figure 2(b) shows the result of the same analysis performed on discharges characterized by a shallow reversal of the toroidal magnetic field,  $q(a) \approx -0.015$ . In this case no peak with  $m = 1$  periodicity is present and the magnetic fluctuations are concentrated at frequencies below 50 kHz, to which the analysis performed by means of poloidal array of probes associates a  $m = 0$  poloidal periodicity. These fluctuations, whose origin is still under debate, are observed to become of smaller amplitude in a deeply reversed discharge, as can be seen in figure 2(a), where the amplitude of the  $m = 1$  peak is observed to be dominant over that of the low frequency  $m = 0$  fluctuations. The  $m = 0$  fluctuations are positioned on an almost continuous linear dispersion relation, in the form  $\omega = (n/R)V_{\text{ph}}$ , with  $\omega = 2\pi f$ , where  $f$  is the frequency,  $n$  is the toroidal mode number and  $V_{\text{ph}}$  is the phase velocity of the fluctuations in the toroidal direction. The measured phase velocity is of the order of 20–30 km s<sup>-1</sup> in the counter toroidal plasma current direction corresponding to the electron diamagnetic direction, which is in good agreement with the plasma flow velocity at the edge of the RFX-mod device

deduced by means of gas puffing imaging diagnostics [28] and is also consistent with the  $E \times B$  flow measured by the Langmuir probes [29].

It is important to note that the  $m = 1$  peak in the  $(n, f)$  plane of figure 2(a) appears to be almost aligned with the linear dispersion relation characterizing the continuum low frequency  $m = 0$  part of the spectrum. This is an indication that the frequency associated with the mode with  $n > 20$  is mainly due to a Doppler effect, as the mode rotates with the plasma. The analysis for different values of  $q(a)$  reveals that the value of  $n$  corresponding to the maximum of the fluctuation amplitude is observed to follow the relation  $n \cdot |q(a)| \approx 1$ . The measured poloidal and toroidal mode numbers thus indicate that the observed high frequency modes correspond to magnetic perturbations resonating at the edge of the plasma column, in the region between the reversal surface and the inner surface of the graphite tiles constituting the first wall of the RFX-mod machine. In the RFP nomenclature these are called externally resonant modes [27]. It must be added that due to the rather narrow range, around 2%, of the explored  $\beta$  values, where the definition  $\beta \equiv \langle n_e T_e \rangle / ((B)^2 / 2\mu_0)$  is used (the brackets  $\langle \rangle$  indicate volume average), the role of  $\beta$  in determining the different dynamics at deep and shallow reversal cannot be experimentally determined.

The measured spectra were compared with those predicted by a linear stability analysis performed by means of the cylindrical code ETAW, already extensively used for RFP calculations [27] and, more recently, successfully benchmarked against the MARS code [31]. The code solves the linear cylindrical resistive incompressible and inviscid single fluid MHD equations, using a spectral formulation and a matrix shooting eigenvalue scheme. Up to two resistive walls are considered for the boundary conditions, with a thin shell approximation. The plasma model is solved inside the first wall and the solution is then matched with the external solution of the vacuum cylindrical Laplace equation, analytically known in terms of modified Bessel functions. For the problem under consideration we have assumed that only one wall is present, which corresponds to a perfect ideal shell at a shell proximity ( $b/a$ ) of about 1.05, i.e. 5% of the plasma minor radius. This choice appears to be the most appropriate, since, as it has been shown by the measurements, the modes rotate at a relatively high speed together with the plasma, and, on the other hand, a metal liner with 1–2 ms magnetic field penetration time is present in the RFX-mod device. Therefore the liner acts as a perfect conductor for these fast rotating modes.

The value of  $\beta$  adopted in the simulation is 2%, comparable to the experimental one for the considered case. In the simulations, two different pressure profiles, shown in figure 3, have been adopted. The two chosen profiles are compared with a typical experimental one in RFX-mod, obtained from density and temperature profiles published in [33, 34], respectively, measured in almost identical discharges. The two profiles for the theoretical estimations are actually intended to represent those corresponding to the minimum and maximum edge gradients measured in the RFX-mod plasmas under the experimental conditions explored here. With these assumptions, we obtained the spectrum of unstable modes given in figure 4(a) for two different  $q$  profiles (deduced by means of the same magnetic profile reconstruction used

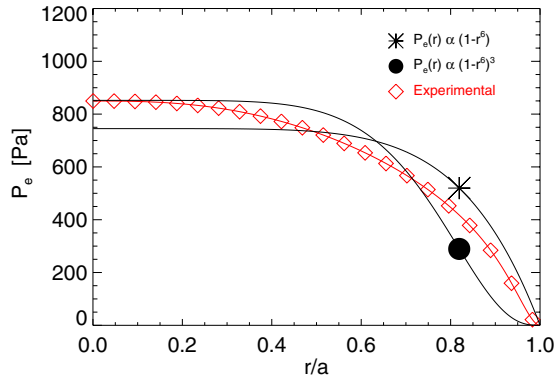


**Figure 3.** Two different radial pressure profiles adopted in the theoretical analysis compared with a typical experimental profile (diamonds).

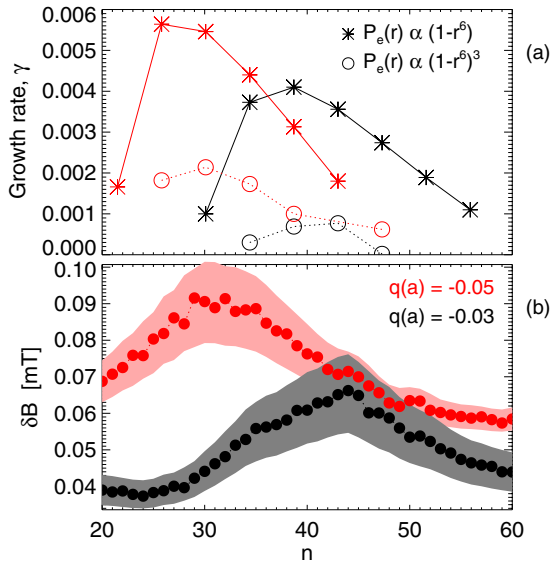


**Figure 4.** (a) Theoretical growth rate for different toroidal mode numbers, corresponding to two  $q(a)$ . Different symbols mark the two different plasma pressure profiles used for the simulation. (b) Experimental  $S(n)$  spectra under the same  $q(a)$  conditions of (a) (experimental spectra are obtained as average over 10 comparable discharges, in terms of  $I_p$ ,  $n_e$  and  $q(a)$ ).

in figure 2(c)), one with a deeper reversal, corresponding to  $q(a) = -0.05$ , in which the spectrum is peaked at a lower  $n$  value ( $n \approx 25$ ), and one at a shallower reversal, with  $q(a) = -0.03$ , with a spectrum peak at  $n \approx 40$ . The theoretical predictions are in good agreement with the experimental toroidal mode number spectra  $S(n)$ , shown in figure 4(b), obtained by integrating the  $S(n, f)$  spectra over frequencies above 30 kHz, which, as discussed above, are those pertaining to the investigated  $m = 1$  modes (in order to obtain the value of the fluctuating magnetic field, magnetic signals have been numerically integrated). In particular, similarly to the experimental results, the toroidal mode number spectrum for a given equilibrium of figure 4(a) shows that the growth rate  $\gamma$  (normalized to the Alfvén time) vanishes for modes resonant close to the stabilizing wall (at low  $n$ 's), and also for

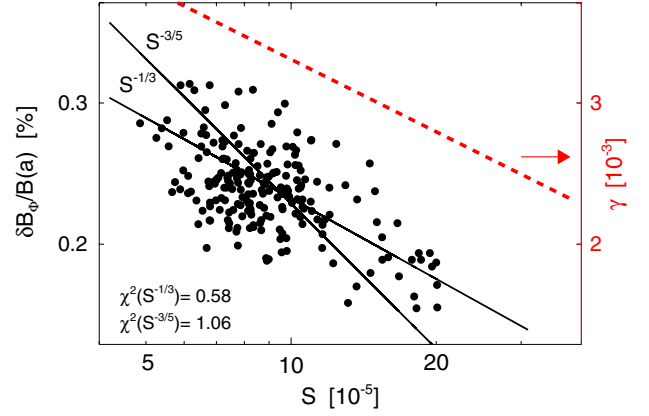


**Figure 5.** Total normalized amplitude of the magnetic perturbation as a function of the Lundquist number  $S$  for a given plasma equilibrium ( $q(a) = -0.03$ ). Two theoretical  $S$  scalings are overplotted: the  $S^{-1/3}$  scaling, predicted for  $g$ -modes, and the  $S^{-3/5}$  scaling, predicted for tearing modes. The results of the  $\chi^2$  test applied to the experimental data for the two scalings are indicated. Dashed line, referring to the right-hand side  $y$ -axis, represents the dependence on  $S$  of the growth rate predicted by the ETAW code for the same plasma equilibrium.

modes resonant close to the reversal of the toroidal magnetic field (at high  $n$ 's), where the effect of the magnetic shear is stronger. As also shown in figure 4(a), the theoretical growth rates at a given  $\beta$  are strongly influenced by the pressure profile. It can be clearly seen that larger edge pressure gradients are associated with larger  $\gamma$  values. Moreover, the results of simulations performed imposing a zero  $\beta$  show that the modes are linearly stable in the absence of pressure. The model also indicates that the growth rates scale as  $\sim S^{-0.3}$  ( $S$  being the Lundquist number), as shown in figure 5, for the plasma equilibrium corresponding to  $q(a) = -0.03$  (chosen as the equilibrium exhibiting a clear  $m = 1$  high frequency activity for which the largest range of  $S$  values is experimentally available), which is very close to the theoretically expected  $S^{-1/3}$  [35]. In the same figure, the theoretical growth rates are compared with the experimental total amplitude of the magnetic fluctuations, obtained by summing the contribution from each single toroidal harmonic. Despite the large dispersion of the experimental points, a scaling close to  $S^{-1/3}$  is fully compatible with the data. For a comparison, the  $S^{-3/5}$  scaling is overplotted in the figure, which would be the expected  $S$  scaling for tearing modes [35]; the results of the  $\chi^2$  test for the two theoretical scalings, indicated in the figure, show that the  $S^{-1/3}$  scaling fits the experimental data better than the  $S^{-3/5}$  one. It must also be said that an interpretation of the observed magnetic fluctuations in terms of tearing modes can be reasonably excluded, as these kinds of modes are observed to only slowly rotate in RFX-mod [36], so that they are easily distinguishable from the high frequency magnetic activity under investigation here. For all the reasons proposed, i.e. the effect of the resonance, the effect of the beta and shear and Lundquist scaling, we can classify these modes as resistive  $g$ . These are interchange-like instabilities which can develop in a RFP at relatively low  $\beta$  values [32], i.e. well below Suydam's limit for ideal interchanges.

As a last point we want to address the problem of nonlinear saturation of these modes. Clearly for this purpose a nonlinear

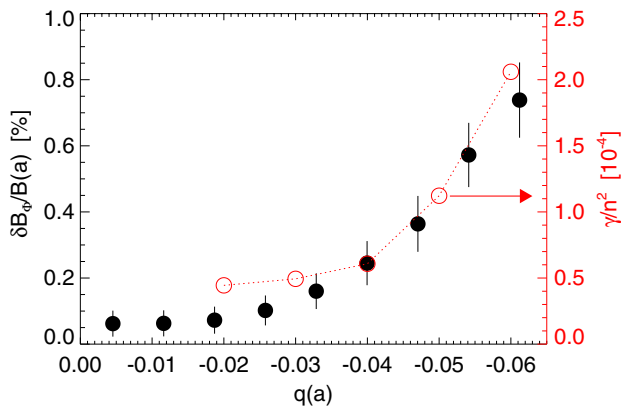


**Figure 6.** Total (normalized) magnetic perturbation  $\delta B_\phi$  induced by the resistive  $g$ -modes as a function of  $q(a)$  (full circles). Theoretical growth rate, normalized to the squared  $n$  values, as a function of  $q(a)$  (open circles).

model would be required (see for example [37]), and/or a model taking into account all the effects which could affect the stability properties of  $g$ -modes extensively described in the literature, with the inclusion of finite Larmor effects, parallel ion viscosity and diamagnetics effects [38, 39, and references therein]. However, we consider a simple quasi-linear model in which the growth rate is balanced by a dissipation mechanism proportional to the squared mode wave number, which is the consequence of having a Laplacian-like dissipation term in the equations. In this case, it is expected that the measured fluctuation amplitude correlates with some quantity which takes into account both the growth rate and the mode number. As shown in figure 6, despite the simplicity of the model, a very good correlation is found between the maximum growth rate divided by the square of the mode number (corresponding to the maximum) at different  $q(a)$  values and the experimental amplitude of the fluctuations. In particular, in figure 6 the amplitude of the total perturbation produced by these modes is observed to reach values up to almost 1% of the equilibrium magnetic field at the edge in deeply reversed discharges. It is worth noting that the magnetic perturbation produced is smaller by only a factor of four than that due to the core resonant dynamo modes, which are essential to sustain the RFP configuration and the Lundquist scaling agrees with the one found for the secondary tearing modes and reported in [40]. Therefore we think that the described phenomenon could play an important role in determining the edge transport properties in RFP plasmas, for which the exact mechanism is still under debate. Future studies are required to better understand why the ‘footprints’ of the linear stability properties are so clearly impressed in the nonlinear saturated state of MHD interchange resistive turbulence in our device. It will also be crucial to analyse possible ways for the control of the resistive  $g$ -modes, as their importance is expected to largely increase in reactor relevant beta conditions.

This work, supported by the European Communities under the contract of Association between EURATOM/ENEA, was carried out within the framework of the European Fusion Development Agreement.

Consorzio RFX-Euratom/ENEA Association © 2010.

## References

- [1] Coppi B. and Keyes E.A. 2003 *Astrophys. J.* **595** 1000
- [2] Xiao F. *et al* 2003 *Geophys. Res. Lett.* **30** 1749
- [3] Sharma A.S. *et al* 2008 *Ann. Geophys.* **26** 955
- [4] Parnowski A.S. *et al* 2007 *Ann. Geophys.* **25** 1391
- [5] Horton W. *et al* 2001 *J. Geophys. Res.—Space Phys.* **106** 18803
- [6] Poli F.M. *et al* 2006 *Phys. Plasmas* **13** 102104
- [7] Menard J.E. *et al* 2006 *Phys. Rev. Lett.* **97** 095002
- [8] Ichiguchi K. *et al* 2003 *Nucl. Fusion* **43** 1101
- [9] Guo H.Y. *et al* 2005 *Phys. Rev. Lett.* **95** 175001
- [10] Connor J.W., Hastie R.J. and Taylor J.B. 1978 *Phys. Rev. Lett.* **40** 396
- [11] Tokar M.Z., Evans T.E., Gupta A., Singh R., Kaw P. and Wolf R.C. 2007 *Phys. Rev. Lett.* **98** 095001
- [12] Ortolani S. and Schnack D.D. 1993 *Magnetohydrodynamics of Plasma relaxation* (Singapore: World Scientific)
- [13] Suydam B.R. 1958 *Proc. 2nd Int. Conf. on Peaceful Uses of Atomic Energy (UN, Geneva, 1958)* vol 31 p 157
- [14] Hender T.H. and Robinson D. 1983 *Proc. 9th Int. Conf. on Plasma Physics and Controlled Nuclear Fusion Research 1982 (Baltimore, MD, 1982)* vol III p 417 (Vienna: IAEA)
- [15] Carreras B. *et al* 1989 *Phys. Fluids B* **1** 1011
- [16] Manheimer W.M. 1980 *Phys. Rev. Lett.* **45** 1249–53
- [17] Wyman M.D. *et al* 2009 *Nucl. Fusion* **49** 015003
- [18] Bruno A., Freidberg J.P. and Hastie R.J. 2003 *Phys. Plasmas* **10** 2330–9
- [19] Bruno A., Freidberg J.P. and Hastie R.J. 2003 *Phys. Plasmas* **10** 2340–9
- [20] Dahlin J.E. and Scheffel J. 2007 *Nucl. Fusion* **47** 1184–8
- [21] Brunsell P.R., Maejima Y., Yagi Y., Hirano Y. and Shimada T. 1994 *Phys. Plasmas* **1** 2297–307
- [22] Sonato P. *et al* 2003 *Fusion Eng. Des.* **66–68** 161–68
- [23] Paccagnella R. *et al* 2006 *Phys. Rev. Lett.* **97** 075001
- [24] Zanca P., Marrelli L., Manduchi G. and Marchiori G. 2007 *Nucl. Fusion* **47** 1425–36
- [25] Serriani G. *et al* 2004 *Rev. Sci. Instrum.* **75** 4338
- [26] Zuin M. *et al* 2009 *Plasma Phys. Control. Fusion* **51** 035012
- [27] Paccagnella R. 1998 *Nucl. Fusion* **38** 1067
- [28] Scarin P. *et al* 2007 *J. Nucl. Mater.* **363–365** 669
- [29] Spolaore M. *et al* 2009 *Phys. Rev. Lett.* **102** 165001
- [30] Beall J.M., Kim Y.C. and Powers E.J. 1982 *J. Appl. Phys.* **53** 3933
- [31] Villone F. *et al* 2008 *Phys. Rev. Lett.* **100** 255005
- [32] Merlin D., Ortolani S., Paccagnella R. and Scapin M. 1989 *Nucl. Fusion* **29** 1153
- [33] Lorenzini R., Terranova D., Auriemma F., Cavazzana R., Innocente P., Martini S., Serriani G. and Zuin M. 2007 *Nucl. Fusion* **47** 1468–75
- [34] Alfier A. and Pasqualotto R. 2007 *Rev. Sci. Instrum.* **78** 013505
- [35] Liu D.H. 1997 *Nucl. Fusion* **37** 1083–93
- [36] Zanca P. 2009 *Plasma Phys. Control. Fusion* **51** 015006
- [37] Battacharjee A. and Hameiri E. 1986 *Phys. Rev. Lett.* **57** 206
- [38] Sydora R.D. *et al* 1986 *Phys. Fluids* **29** 2871
- [39] Zhu P. *et al* 2008 *Phys. Rev. Lett.* **101** 085005
- [40] Lorenzini R. *et al* 2009 *Nature Phys.* **5** 570